ZAMM · Z. Angew. Math. Mech. **92**, No. 11 – 12, 910 – 920 (2012) / **DOI** 10.1002/zamm.201200028

On the use of sampling surfaces method for solution of 3D elasticity problems for thick shells

G. M. Kulikov* **and S. V. Plotnikova**

Department of Applied Mathematics and Mechanics, Tambov State Technical University, Sovetskaya Street, 106, 392000 Tambov, Russia

Received 11 February 2012, revised 22 April 2012, accepted 31 May 2012
Published online 5 July 2012

Key words Elasticity, 3D static shell problems, higher order shell models, sampling surfaces.

This paper presents a simple and effective method of solving the 3D elasticity problems for thick shells. It is based on the new concept of sampling surfaces (S-surfaces) inside the shell body. According to this concept, we introduce N not equally located S-surfaces parallel to the midsurface and choose displacements of these surfaces as basic shell unknowns. Such choice allows one to represent the governing equations of the proposed higher order shell model in a very compact form and to solve the 3D static problems for thick plates and shells efficiently.

1 Introduction

A conventional way of developing the refined models of shells consists in the expansion of displacements into power series with respect to the transverse coordinate, which is referred to the direction normal to the midsurface of the shell. For the approximate representation of the displacement field, it is possible to use finite segments of power series because the principal purpose of the shell theory consists in the derivation of approximate solutions of the 3D elasticity theory. The idea of this approach can be traced back to Cauchy [1]. Such a way has been extensively utilized for development of plate and shell theories accounting for thickness stretching [2–7]. The shell theory can be also formulated by using the expansion of displacements into series in the Legendre polynomials with respect to the thickness coordinate [8]. For a complete review, the reader is referred to survey articles and textbooks [9–17]. However, the implementation of these approaches for thick shells is not straightforward since it is necessary to retain a large number of terms in corresponding expansions to obtain the comprehensive results.

In the present paper, it is discussed an alternative way of developing the shell theory through the use of a new method of S-surfaces proposed recently by the authors [18, 19]. As S-surfaces Ω^1, $\Omega^2, \ldots, \Omega^N$, it was suggested to choose outer surfaces and any inner surfaces parallel to the midsurface, in order to introduce displacement vectors $\mathbf{u}^1$, $\mathbf{u}^2, \ldots, \mathbf{u}^N$ of these surfaces as basic kinematic variables. Such choice of displacements in conjunction with the use of Lagrange polynomials of degree $N-1$ in the thickness direction permits one to represent governing equations of the higher order shell theory in a very compact form and derive strain-displacement equations, which describe exactly all rigid-body motions of the shell in any convected curvilinear coordinate system.

Later, it was established that a proposed polynomial interpolation does not work properly with Lagrange polynomials of *high* degree because Runge's phenomenon can occur, which yields the wild oscillation at the edges of the interval when one deals with any specific functions [20]. If the number of nodes is increased then the oscillations become even larger. However, the use of Chebyshev polynomial nodes [20] can help to improve essentially the behaviour of Lagrange polynomials of high degree for which the error will go to zero as $N \to \infty$. This fact gives an opportunity to derive the 3D solutions for thick plates and shells with a prescribed accuracy utilizing a large number of not equally spaced S-surfaces.

2 Kinematic description of undeformed shell

Consider a thick shell of the thickness h. Let the midsurface Ω be described by orthogonal curvilinear coordinates θ_1 and θ_2, which are referred to the lines of principal curvatures of its surface. The coordinate θ_3 is oriented along the unit vector $\boldsymbol{a}_3 = \mathbf{e}_3$ normal to the midsurface Ω. Introduce the following notations: $\mathbf{r} = \mathbf{r}(\theta_1, \theta_2)$ is the position vector of any point of

* Corresponding author E-mail: kulikov@apmath.tstu.ru

the midsurface; $\boldsymbol{a}_\alpha$ are the base vectors of the midsurface defined as

$$\boldsymbol{a}_\alpha = \mathbf{r}_{,\alpha} = A_\alpha \mathbf{e}_\alpha, \tag{1}$$

where $\mathbf{e}_\alpha$ are the orthonormal base vectors; A_α are the coefficients of the first fundamental form; $\mathbf{R} = \mathbf{r} + \theta_3 \mathbf{e}_3$ is the position vector of any point in the shell body; $\mathbf{R}^I = \mathbf{r} + \theta_3^I \mathbf{e}_3$ are the position vectors of S-surfaces located at the Chebyshev polynomial nodes (Fig. 1), which are chosen inside the interval $(-h/2,\ h/2)$; θ_3^I are the transverse coordinates of S-surfaces expressed as in [20]

$$\theta_3^I = -\frac{h}{2} \cos\left(\pi \frac{2I-1}{2N}\right), \tag{2}$$

where the index I identifies the belonging of any quantity to the S-surfaces and takes values $1,\ 2,\ \ldots,\ N$; $\mathbf{g}_i$ are the base vectors in the shell body given by

$$\mathbf{g}_\alpha = \mathbf{R}_{,\alpha} = A_\alpha c_\alpha \mathbf{e}_\alpha, \quad \mathbf{g}_3 = \mathbf{R}_{,3} = \mathbf{e}_3, \tag{3}$$

$$c_1 = \mu_1^1 = 1 + k_1\theta_3, \quad c_2 = \mu_2^2 = 1 + k_2\theta_3,$$

where μ_α^β are the components of the shifter tensor in orthogonal curvilinear coordinate system such that $\mu_1^2 = \mu_2^1 = 0$; k_α are the principal curvatures of the midsurface; $\mathbf{g}_i^I$ are the base vectors of S-surfaces defined as

$$\mathbf{g}_\alpha^I = \mathbf{R}_{,\alpha}^I = A_\alpha c_\alpha^I \mathbf{e}_\alpha, \quad \mathbf{g}_3^I = \mathbf{e}_3, \tag{4}$$

$$c_\alpha^I = c_\alpha(\theta_3^I) = 1 + k_\alpha \theta_3^I.$$

Here and in the following developments, $(\ldots)_{,i}$ stands for the partial derivatives with respect to coordinates θ_i; Greek indices $\alpha,\ \beta$ range from 1 to 2; Latin indices $i,\ j,\ k,\ m$ range from 1 to 3.

3 Kinematic description of deformed shell

A position vector of the deformed shell is written as

$$\bar{\mathbf{R}} = \mathbf{R} + \mathbf{u}, \tag{5}$$

where $\mathbf{u}$ is the displacement vector, which is always measured in accordance with the total Lagrangian formulation from the initial configuration to the current configuration directly. In particular, the position vectors of S-surfaces (Fig. 2) are

$$\bar{\mathbf{R}}^I = \mathbf{R}^I + \mathbf{u}^I, \quad \mathbf{u}^I = \mathbf{u}(\theta_3^I), \tag{6}$$

where $\mathbf{u}^I\ (\theta_1,\ \theta_2)$ are the displacement vectors of S-surfaces.

The base vectors in the current shell configuration are defined as

$$\bar{\mathbf{g}}_i = \bar{\mathbf{R}}_{,i} = \mathbf{g}_i + \mathbf{u}_{,i}. \tag{7}$$

In particular, the base vectors of S-surfaces of the deformed shell are

$$\bar{\mathbf{g}}_\alpha^I = \bar{\mathbf{R}}_{,\alpha}^I = \mathbf{g}_\alpha^I + \mathbf{u}_{,\alpha}^I, \quad \bar{\mathbf{g}}_3^I = \bar{\mathbf{g}}_3(\theta_3^I) = \mathbf{e}_3 + \boldsymbol{\beta}^I, \tag{8}$$

$$\boldsymbol{\beta}^I = \mathbf{u}_{,3}(\theta_3^I), \tag{9}$$

where $\boldsymbol{\beta}^I\ (\theta_1,\ \theta_2)$ are the values of the derivative of the displacement vector with respect to coordinate θ_3 at S-surfaces.

The Green-Lagrange strain tensor (see e.g. [21, 22]) can be expressed as

$$2\varepsilon_{ij} = \frac{1}{A_i A_j c_i c_j}(\bar{\mathbf{g}}_i \cdot \bar{\mathbf{g}}_j - \mathbf{g}_i \cdot \mathbf{g}_j), \tag{10}$$

where $A_3 = 1$ and $c_3 = 1$. In particular, the Green-Lagrange strain components at S-surfaces are

$$2\varepsilon_{ij}^I = 2\varepsilon_{ij}(\theta_3^I) = \frac{1}{A_i A_j c_i^I c_j^I}(\bar{\mathbf{g}}_i^I \cdot \bar{\mathbf{g}}_j^I - \mathbf{g}_i^I \cdot \mathbf{g}_j^I). \tag{11}$$

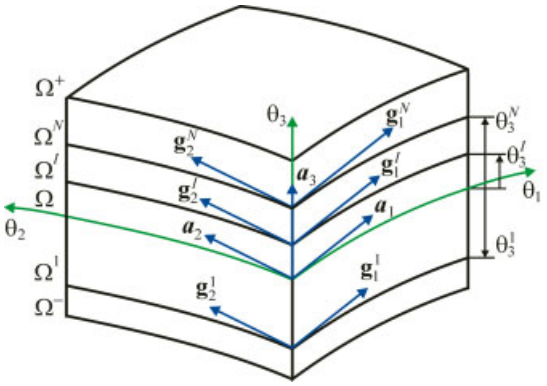

Fig. 1 (online colour at: www.zamm-journal.org) Geometry of the shell.

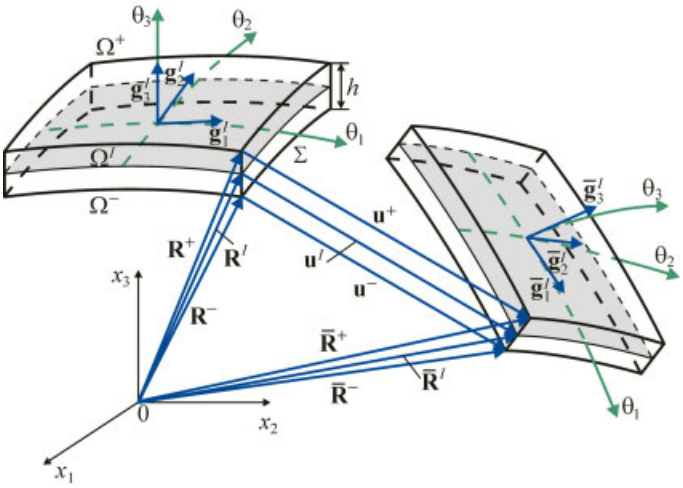

Fig. 2 (online colour at: www.zamm-journal.org) Initial and current configurations of the shell.

Substituting (4) and (8) into strain-displacement relationships (11) and discarding the non-linear terms, one derives

$$2\varepsilon^I_{\alpha\beta} = \frac{1}{A_\alpha c^I_\alpha}\mathbf{u}^I_{,\alpha}\cdot\mathbf{e}_\beta + \frac{1}{A_\beta c^I_\beta}\mathbf{u}^I_{,\beta}\cdot\mathbf{e}_\alpha,$$

$$2\varepsilon^I_{\alpha 3} = \boldsymbol{\beta}^I\cdot\mathbf{e}_\alpha + \frac{1}{A_\alpha c^I_\alpha}\mathbf{u}^I_{,\alpha}\cdot\mathbf{e}_3, \quad \varepsilon^I_{33} = \boldsymbol{\beta}^I\cdot\mathbf{e}_3. \tag{12}$$

Next, we represent the displacement vectors $\mathbf{u}^I$ and $\boldsymbol{\beta}^I$ in the reference surface frame $\mathbf{e}_i$ as follows:

$$\mathbf{u}^I = \sum_i u^I_i\mathbf{e}_i, \quad \boldsymbol{\beta}^I = \sum_i \beta^I_i\mathbf{e}_i. \tag{13}$$

Using (13) and formulas for the derivatives of unit vectors $\mathbf{e}_i$ with respect to orthogonal curvilinear coordinates (see e.g. [1])

$$\frac{1}{A_\alpha}\mathbf{e}_{\alpha,\alpha} = -B_\alpha\mathbf{e}_\beta - k_\alpha\mathbf{e}_3, \qquad \frac{1}{A_\alpha}\mathbf{e}_{\beta,\alpha} = B_\alpha\mathbf{e}_\alpha,$$

$$\frac{1}{A_\alpha}\mathbf{e}_{3,\alpha} = k_\alpha\mathbf{e}_\alpha, \qquad B_\alpha = \frac{1}{A_\alpha A_\beta}A_{\alpha,\beta} \quad (\beta\neq\alpha), \tag{14}$$

one obtains

$$\frac{1}{A_\alpha}\mathbf{u}^I_{,\alpha} = \sum_i \lambda^I_{i\alpha}\mathbf{e}_i, \tag{15}$$

where

$$\lambda^I_{\alpha\alpha} = \frac{1}{A_\alpha}u^I_{\alpha,\alpha} + B_\alpha u^I_\beta + k_\alpha u^I_3, \quad \lambda^I_{\beta\alpha} = \frac{1}{A_\alpha}u^I_{\beta,\alpha} - B_\alpha u^I_\alpha \qquad (\beta\neq\alpha),$$

$$\lambda^I_{3\alpha} = \frac{1}{A_\alpha}u^I_{3,\alpha} - k_\alpha u^I_\alpha. \tag{16}$$

Substitution of presentations (13) and (15) in strain-displacement relationships (12) yields the component form of these relationships

$$2\varepsilon^I_{\alpha\beta} = \frac{1}{c^I_\beta}\lambda^I_{\alpha\beta} + \frac{1}{c^I_\alpha}\lambda^I_{\beta\alpha},$$

$$2\varepsilon^I_{\alpha 3} = \beta^I_\alpha + \frac{1}{c^I_\alpha}\lambda^I_{3\alpha}, \qquad \varepsilon^I_{33} = \beta^I_3. \tag{17}$$

4 Displacement and strain distributions in thickness direction

Up to this moment, no assumptions concerning the distribution of displacements and strains through the thickness of the shell have been made. We start now with the first fundamental assumption of the proposed higher order shell theory. Let us assume that the displacement field is approximated in the thickness direction according to the following law:

$$u_i = \sum_I L^I u_i^I, \tag{18}$$

where $L^I\,(\theta_3)$ are the Lagrange polynomials of degree $N-1$ expressed as

$$L^I = \prod_{J\neq I} \frac{\theta_3 - \theta_3^J}{\theta_3^I - \theta_3^J} \tag{19}$$

such that $L^I\left(\theta_3^J\right) = 1$ for $J = I$ and $L^I\left(\theta_3^J\right) = 0$ for $J \neq I$.

The use of relations (9), (13), and (18) leads to

$$\beta_i^I = \sum_J M^J(\theta_3^I) u_i^J, \tag{20}$$

where $M^I = L^I_{,3}$ are the polynomials of degree $N-2$; their values on S-surfaces can be written as

$$M^J\left(\theta_3^I\right) = \frac{1}{\theta_3^J - \theta_3^I} \prod_{K\neq I,\,J} \frac{\theta_3^I - \theta_3^K}{\theta_3^J - \theta_3^K} \quad (J \neq I),$$

$$M^I\left(\theta_3^I\right) = -\sum_{J\neq I} M^J\left(\theta_3^I\right), \tag{21}$$

where I, J, $K = 1, 2, \ldots, N$. Thus, the key functions β_i^I of the proposed higher order shell theory are represented according to (20) as a linear combination of displacements of S-surfaces u_i^J.

The following step consists in a choice of consistent approximation of strains through the thickness of the shell. It is apparent that the strain distribution should be chosen similar to the displacement distribution (18), that is,

$$\varepsilon_{ij} = \sum_I L^I \varepsilon_{ij}^I. \tag{22}$$

It is necessary to note that strain components (17) and (22) are objective, i.e., they represent exactly all rigid-body motions of the shell in any convected curvilinear coordinate system. It can be verified following a technique developed in [23, 24].

5 Total potential energy

Substituting strains (22) into the total potential energy and introducing stress resultants [18]

$$H_{ij}^I = \int_{-h/2}^{h/2} \sigma_{ij} L^I c_1 c_2 d\theta_3, \tag{23}$$

one obtains

$$\Pi = \iint_\Omega \left[\frac{1}{2} \sum_I \sum_{i,j} H_{ij}^I \varepsilon_{ij}^I - \sum_i \left(c_1^+ c_2^+ p_i^+ u_i^+ - c_1^- c_2^- p_i^- u_i^- \right) \right] A_1 A_2 d\theta_1 d\theta_2 - W_\Sigma\,, \tag{24}$$

where p_i^- and p_i^+ are the loads acting on the bottom and top surfaces Ω^- and Ω^+; $c_\alpha^- = 1 - k_\alpha h/2$ and $c_\alpha^+ = 1 + k_\alpha h/2$ are the components of the shifter tensor at outer surfaces; $u_i^- = u_i(-h/2)$ and $u_i^+ = u_i(h/2)$ are the displacements at outer surfaces; W_Σ is the work done by external loads applied to the boundary surface Σ (see Fig. 2).

For simplicity, we consider the case of linear elastic materials, which are described by the generalized Hooke's law:

$$\sigma_{ij} = \sum_{k,m} C_{ijkm}\varepsilon_{km}, \tag{25}$$

where C_{ijkm} are the components of the material tensor.

The use of relations (22) and (25) in (23) yields

$$H_{ij}^I = \sum_J \sum_{k,m} D_{ijkm}^{IJ}\varepsilon_{km}^J, \tag{26}$$

where

$$D_{ijkm}^{IJ} = C_{ijkm} \int_{-h/2}^{h/2} L^I L^J c_1 c_2 d\theta_3. \tag{27}$$

6 Numerical examples

The performance of the higher order shell theory developed is evaluated by using several analytical solutions of the 3D elasticity extracted from the literature.

6.1 Rectangular plate under sinusoidal loading

Consider first a simply supported rectangular plate subjected to the sinusoidally distributed pressure load as shown in Fig. 3. To satisfy the boundary conditions, we search an analytical solution of the problem as follows:

$$u_1^I = u_{10}^I \cos\frac{\pi\theta_1}{a}\sin\frac{\pi\theta_2}{b}, \quad u_2^I = u_{20}^I \sin\frac{\pi\theta_1}{a}\cos\frac{\pi\theta_2}{b},$$
$$u_3^I = u_{30}^I \sin\frac{\pi\theta_1}{a}\sin\frac{\pi\theta_2}{b}, \tag{28}$$

where a and b are the plate dimensions.

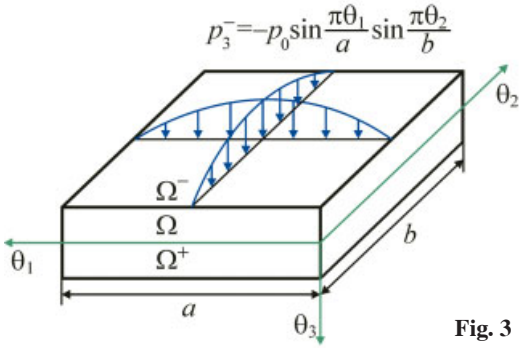

Fig. 3 (online colour at: www.zamm-journal.org) Simply supported rectangular plate.

Inserting displacements (28) into the total potential energy (24) with $W_\Sigma = 0$ and taking into account Eqs. (16), (17) and (26), one finds

$$\Pi = \Pi(u_{i0}^I). \tag{29}$$

Invoking further the principle of the minimum total potential energy, we arrive at the system of linear algebraic equations of order $3N$:

$$\frac{\partial\Pi}{\partial u_{i0}^I} = 0, \tag{30}$$

which is solved by using a method of Gaussian elimination.

The described algorithm was performed with the Symbolic Math Toolbox, which incorporates symbolic computations into the numeric environment of MATLAB. This gave the possibility to derive the exact solutions of 3D elasticity for thick homogeneous shells with a prescribed accuracy.

To compare the results derived with Vlasov's closed-form solution [25], the following dimensionless variables are introduced:

$$S_{11} = 10h^2\sigma_{11}(a/2, b/2, z)/p_0a^2, \quad S_{12} = 10h^2\sigma_{12}(0, 0, z)/p_0a^2,$$
$$S_{13} = 10h\sigma_{13}(0, b/2, z)/p_0a, \quad S_{33} = \sigma_{33}(a/2, b/2, z)/p_0,$$
$$U_3 = 100Eh^3u_3(a/2, b/2, z)/p_0a^4, \quad z = \theta_3/h. \tag{31}$$

Table 1 Results for a thick square plate ($a/h = 2$).

Variant	$U_3(0)$	$S_{11}(-0.5)$	$S_{11}(0.5)$	$S_{12}(-0.5)$	$S_{12}(0.5)$	$S_{13}(0)$	$S_{33}(0)$
$N = 3$	5.6107	−2.6835	1.6435	0.8298	−0.9225	1.5962	0.44381
$N = 5$	6.0423	−3.0275	2.0663	1.0453	−1.1191	2.3071	0.48013
$N = 7$	6.0466	−3.0139	2.0786	1.0458	−1.1194	2.2764	0.47544
$N = 9$	6.0466	−3.0136	2.0788	1.0458	−1.1194	2.2769	0.47553
Vlasov	6.0466	−3.0136	2.0788	1.0458	−1.1194	2.2769	0.47553

The mechanical and geometrical parameters of the isotropic plate are taken to be $E = 10^7$, $\nu = 0.3$, and $a = b = 1$. The data listed in Tables 1 and 2 show that the proposed S-surfaces method permits one to derive the exact solution for the thick plate with a prescribed accuracy utilizing a sufficient number of S-surfaces. Figure 4 presents the distribution of stresses in the thickness direction in the case of using seven S-surfaces for different values of the slenderness ratio a/h. The results demonstrate the high potential of the proposed higher order shell theory. This is due to the fact that boundary conditions for transverse stresses on the bottom and top surfaces of the plate are satisfied precisely without integration of the equilibrium equations of elasticity, i.e., only constitutive equations (25) are employed. Figure 5 displays additionally the logarithmic

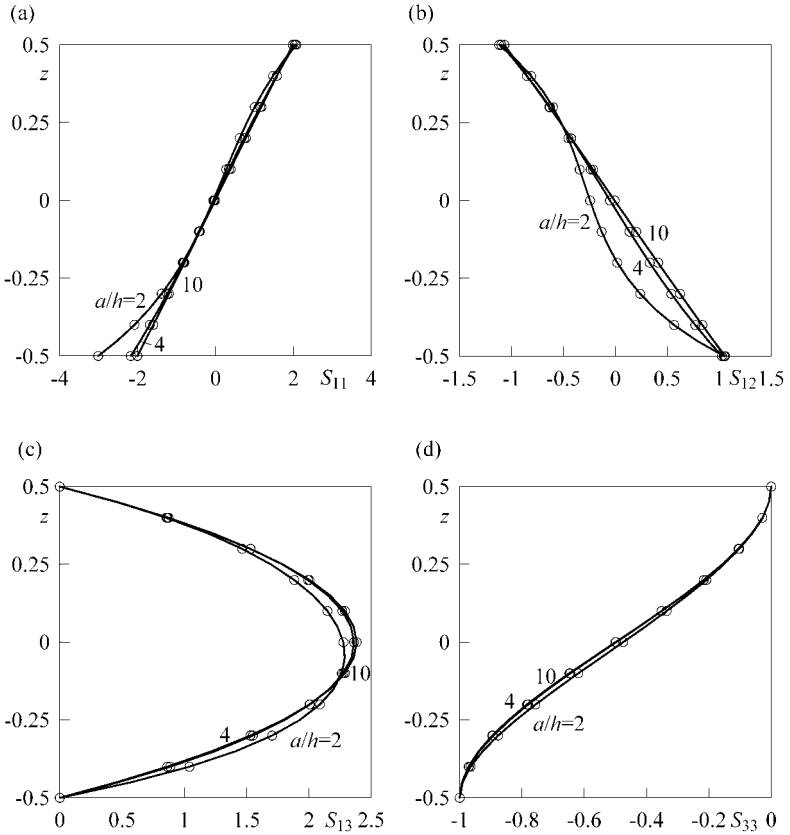

Fig. 4 Distribution of stresses S_{11}, S_{12}, S_{13}, and S_{33} through the thickness of the plate: Vlasov's solution (○) and present higher order shell theory for $N = 7$ (—).

Table 2 Results for a thick plate ($a/h = 4$) with $N = 7$ and a thin plate ($a/h = 100$) with $N = 5$.

a/h	S-surfaces method				Vlasov's solution [25]			
	$U_3(0)$	$S_{11}(-0.5)$	$S_{12}(-0.5)$	$S_{13}(0)$	$U_3(0)$	$S_{11}(-0.5)$	$S_{12}(-0.5)$	$S_{13}(0)$
4	3.6630	−2.1746	1.0267	2.3619	3.6630	−2.1746	1.0267	2.3619
100	2.8040	−1.9760	1.0638	2.3873	2.8040	−1.9760	1.0638	2.3873

errors $\delta_i(-h/2)$ and $\delta_i(h/2)$, which help to assess the accuracy of fulfilling the boundary conditions for transverse stresses on outer surfaces of the plate with $a/h = 2$ and $a/h = 4$. It is necessary to note that the enhanced S-surfaces method provides the monotonic convergence that is impossible with equally spaced S-surfaces [18, 19].

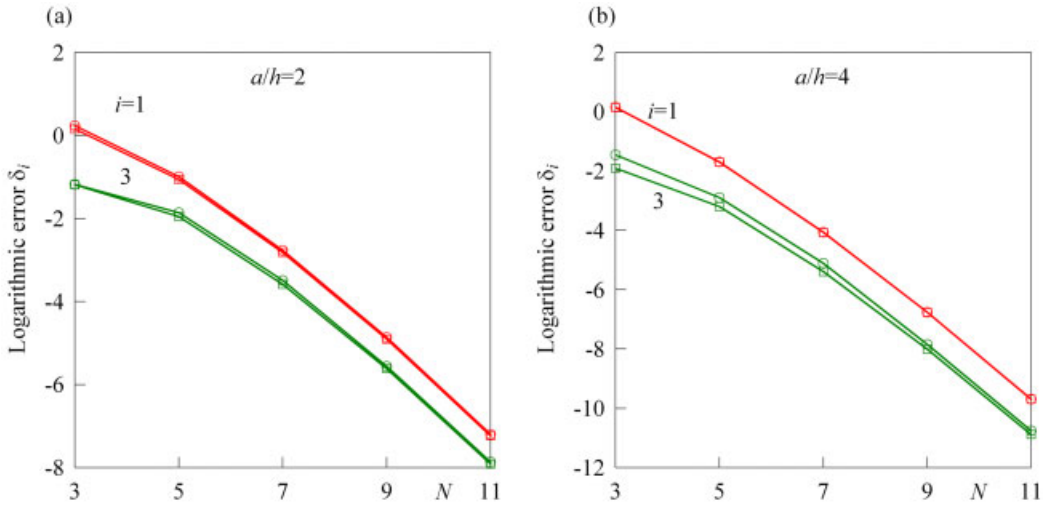

Fig. 5 (online colour at: www.zamm-journal.org) Accuracy of satisfying the boundary conditions $\delta_i(-h/2)$ and $\delta_i(h/2)$ on bottom (○) and top (□) surfaces for thick plates: (a) $a/h = 2$ and (b) $a/h = 4$, where $\delta_i = \lg\left|S_{i3}^{\text{Vlasov}} - S_{i3}^{\text{Present}}\right|$.

6.2 Cylindrical shell under sinusoidal loading

Next, we study a simply supported cylindrical shell with $L/R = 4$ subjected to the sinusoidal loading acting on the inner surface

$$p_3^- = -p_0 \sin\frac{\pi\theta_1}{L}\cos 4\theta_2, \tag{32}$$

where L and R are the length and radius of the shell; θ_1 and θ_2 are the axial and circumferential coordinates of the midsurface. The shell is made of the unidirectional composite with the fibers oriented in the circumferential direction. The material properties are chosen to be $E_1 = 25 \cdot 10^6$, $E_2 = E_3 = 10^6$, $G_{12} = G_{13} = 5 \cdot 10^5$, $G_{23} = 2 \cdot 10^5$, $\nu_{12} = \nu_{13} = \nu_{23} = 0.25$. The stiffness coefficients C_{ijkm} are calculated by means of equations [16].

The analytical solution of the problem satisfying the boundary conditions can be written as

$$u_1^I = u_{10}^I \cos\frac{\pi\theta_1}{L}\cos 4\theta_2, \quad u_2^I = u_{20}^I \sin\frac{\pi\theta_1}{L}\sin 4\theta_2,$$

$$u_3^I = u_{30}^I \sin\frac{\pi\theta_1}{L}\cos 4\theta_2. \tag{33}$$

As in a previous section, one can employ the MATLAB framework to find the exact solution of the problem. To compare the results derived with Varadan's analytical solution [26], we use the dimensionless variables

$$S_{11} = 100h^2\sigma_{11}(L/2,\, 0,\, z)/p_0R^2, \quad S_{22} = 10h^2\sigma_{22}(L/2,\, 0,\, z)/p_0R^2,$$

$$S_{12} = 100h^2\sigma_{12}(0,\, \pi/8,\, z)/p_0R^2, \quad S_{13} = 100h\sigma_{13}(0,\, 0,\, z)/p_0R,$$

$$S_{23} = 10h\sigma_{23}(L/2,\, \pi/8,\, z)/p_0R, \quad S_{33} = \sigma_{33}(L/2,\, 0,\, z)/p_0,$$

$$U_3 = 10E_1h^3u_3(L/2,\, 0,\, z)/p_0R^4, \quad z = \theta_3/h. \tag{34}$$

The data listed in Tables 3 and 4 demonstrate again the high potential of the developed S-surfaces method. Figure 6 presents the distribution of stresses in the thickness direction using 11 S-surfaces for different values of the slenderness ratio R/h. It is seen that the boundary conditions on outer surfaces of the shell are satisfied correctly in spite of applying constitutive equations (25); see also Fig. 7.

Table 3 Results for a thick cylinder ($R/h = 2$).

Variant	$U_3(0)$	$S_{11}\,(0.5)$	$S_{22}\,(0.5)$	$S_{12}\,(-0.5)$	$S_{13}\,(0)$	$S_{23}\,(0)$	$S_{33}(0)$
$N = 5$	7.2715	0.9136	4.2904	−1.5967	1.5135	−2.1281	−0.37744
$N = 7$	7.4825	1.1672	5.0419	−1.7408	1.4955	−1.9869	−0.36603
$N = 9$	7.5005	1.2870	5.1406	−1.7592	1.5031	−2.0730	−0.37617
$N = 11$	7.5030	1.3236	5.1592	−1.7606	1.5037	−2.0518	−0.37362
$N = 13$	7.5031	1.3316	5.1629	−1.7607	1.5035	−2.0561	−0.37416
Varadan	7.503	1.332	5.163	−1.761	1.504	−2.056	−0.37

Table 4 Results for a thick cylinder ($R/h = 4$) with $N = 11$ and a thin cylinder ($R/h = 100$) with $N = 7$.

R/h	S-surfaces method				Varadan's solution [26]			
	$U_3(0)$	$S_{22}\,(0.5)$	$S_{13}(0)$	$S_{23}(0)$	$U_3(0)$	$S_{22}\,(0.5)$	$S_{13}(0)$	$S_{23}\,(0)$
4	2.7828	4.8593	0.98682	−2.9895	2.783	4.859	0.987	−2.990
100	0.5170	3.8431	0.39300	−3.8590	0.5170	3.843	0.393	−3.859

6.3 Spherical shell under inner pressure

Finally, we study an isotropic spherical shell subjected to inner pressure p_0. The mechanical and geometrical parameters are taken to be $E = 10^7$, $\nu = 0.3$, and $R = 10$. To verify the results derived, we invoke Lamé's closed-form solution [27], which can be written as

$$u_r = \frac{p_0a^3}{E\,(b^3 - a^3)}\left[(1-2\nu)\,r + (1+\nu)\,\frac{b^3}{2r^2}\right], \qquad \varepsilon_r = \frac{du_r}{dr},$$

$$\varepsilon_\theta = \varepsilon_\varphi = \frac{u_r}{r}, \qquad a = R - \frac{1}{2}h, \qquad b = R + \frac{1}{2}h, \tag{35}$$

where r is the radial distance from a point to the origin; R is the radius of the midsurface. As in previous examples, we introduce the dimensionless variables

$$S_{11} = 10h\sigma_{11}(\,z)/p_0R, \quad S_{33} = \sigma_{33}(z)/p_0,$$

$$U_3 = 10Ehu_3(\,z)/p_0R^2, \quad z = \theta_3/h \tag{36}$$

and search the analytical solution using the MATLAB framework in the following form: $u_\alpha^I = 0$ and $u_3^I = u_{30}^I$.

The data listed in Tables 5 and 6 show again an excellent performance of the higher order shell theory developed even in the case of choosing seven S-surfaces. Figure 8 displays the distribution of normal stress components through the thickness of the shell by utilizing seven S-surfaces.

Table 5 Results for a thick sphere ($R/h = 2$).

Variant	$U_3(-0.5)$	$U_3(0)$	$U_3(0.5)$	$S_{11}\,(-0.5)$	$S_{11}\,(0.5)$	$S_{33}\,(-0.5)$	$S_{33}\,(0)$
$N = 3$	3.4745	2.2865	1.7923	5.2494	2.4878	−0.5979	−0.37813
$N = 5$	3.5222	2.2996	1.8080	4.6091	2.0903	−0.9783	−0.25751
$N = 7$	3.5223	2.2999	1.8080	4.5681	2.0671	−0.9991	−0.26274
$N = 9$	3.5223	2.2999	1.8080	4.5665	2.0663	−0.9999	−0.26260
$N = 11$	3.5223	2.2999	1.8080	4.5664	2.0663	−1.0000	−0.26260
Lamé	3.5223	2.2999	1.8080	4.5663	2.0663	−1.0000	−0.26260

Table 6 Results for a thick sphere ($R/h = 4$) with $N = 9$ and a thin sphere ($R/h = 100$) with $N = 5$.

R/h	S-surfaces method				Lamé's solution [27]			
	$U_3(0)$	$S_{11}\,(-0.5)$	$S_{11}\,(0.5)$	$S_{33}\,(0)$	$U_3(0)$	$S_{11}\,(-0.5)$	$S_{11}\,(0.5)$	$S_{33}\,(0)$
4	2.9446	4.5823	3.3323	−0.37661	2.9446	4.5823	3.3323	−0.37661
100	3.4799	4.9753	4.9253	−0.49500	3.4799	4.9753	4.9253	−0.49500

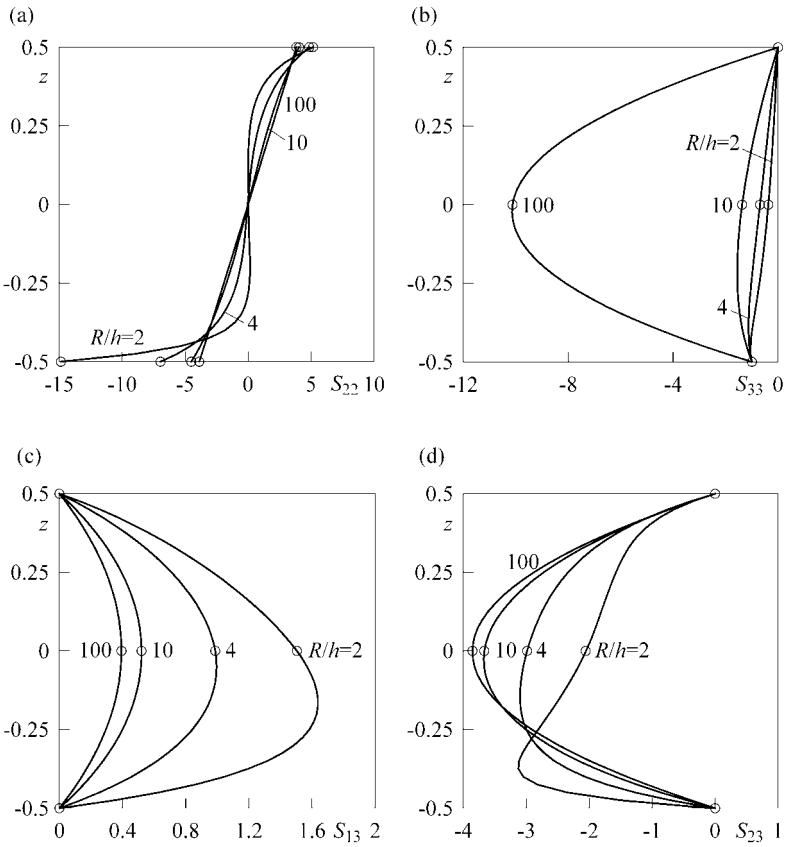

Fig. 6 Distribution of stresses S_{22}, S_{33}, S_{13}, and S_{23} through the thickness of the cylindrical shell: Varadan's solution (○) and present higher order shell theory for $N = 11$ (—).

7 Conclusions

An effective method of solving the 3D elasticity problems for thick shells has been proposed. It is based on the new concept of S-surfaces located at Chebyshev polynomial nodes inside the shell body. This method permits the use of 3D constitutive equations and leads to the exact solutions of 3D elasticity problems for thick shells with a prescribed accuracy employing a sufficiently large number of S-surfaces.

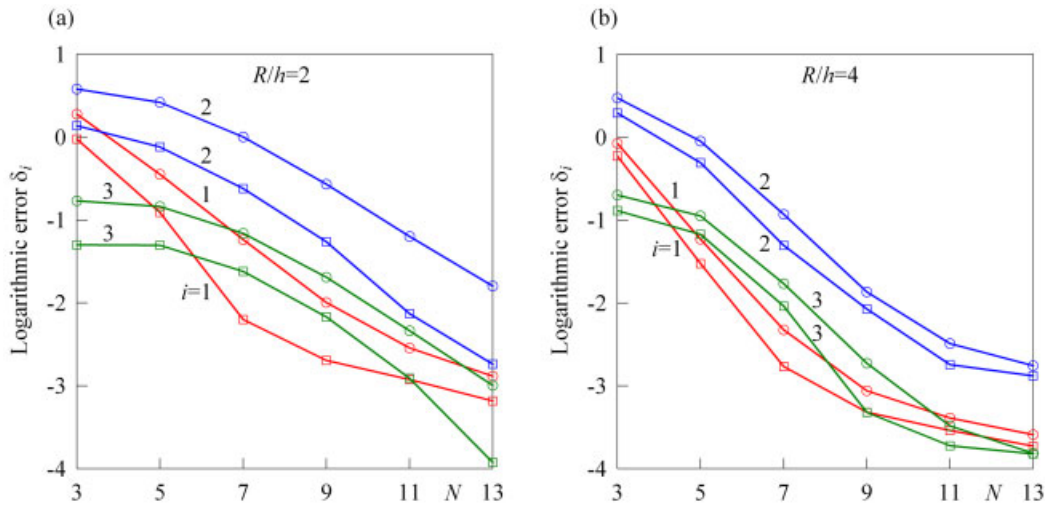

Fig. 7 (online colour at: www.zamm-journal.org) Accuracy of satisfying the boundary conditions $\delta_i(-h/2)$ and $\delta_i(h/2)$ on bottom (○) and top (□) surfaces for thick cylindrical shells: (a) $R/h = 2$ and (b) $R/h = 4$, where $\delta_i = \lg\left|S_{i3}^{\text{Varadan}} - S_{i3}^{\text{Present}}\right|$.

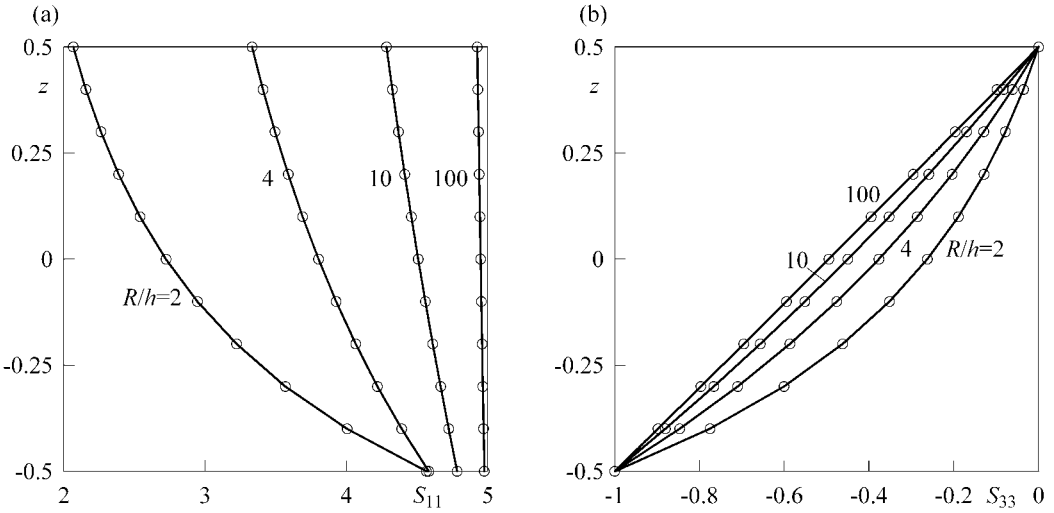

Fig. 8 Distribution of stresses S_{11} and S_{33} through the thickness of the spherical shell: Lamé's solution (○) and present higher order shell theory for $N = 7$ (—).

Acknowledgements This work was supported by Russian Ministry of Education and Science under Grant No 1.472.2011.

References

[1] V. V. Novozhilov, The Theory of Thin Shells (Noordhoff Ltd, Groningen, 1959).
[2] L. Librescu, Elastostatics and Kinetics of Anisotropic and Heterogeneous Shell-Type Structures (Noordhoff Int. Publishing, Leyden, 1975).
[3] K. H. Lo, R. M. Christensen, and E. M. Wu, A higher-order theory of plate deformation. Part I. Homogeneous plates, J. Appl. Mech. **44**, 663–668 (1977).
[4] E. I. Grigolyuk and G. M. Kulikov, General direction of development of the theory of multilayered shells, Mech. Compos. Mater. **24**, 231–241 (1988).
[5] R. Kienzler, On consistent plate theories, Arch. Appl. Mech. **72**, 229–247 (2002).
[6] E. Carrera, Theories and finite elements for multilayered plates and shells: A unified compact formulation with numerical assessment and benchmarking, Arch. Comput. Methods Eng. **10**, 215–296 (2003).
[7] W. B. Krätzig and D. Jun, On "best" shell models – from classical shells, degenerated and multi-layered concepts to 3D, Arch. Appl. Mech. **73**, 1–25 (2003).

[8] I. N. Vekua, Shell Theory: General Methods of Construction (Pitman Advanced Publ. Program, Boston, 1985).
[9] E. I. Grigolyuk and E. A. Kogan, State of the art of the theory of multilayer shells, Int. Appl. Mech. **8**, 583–595 (1972).
[10] R. K. Kapania, A review on the analysis of laminated shells, J. Pressure Vessel Technol. **111**, 88-96 (1989).
[11] A. K. Noor and W. S. Burton, Assessment of computational models for multilayered composite shells, Appl. Mech. Rev. **43**, 67–97 (1990).
[12] J. N. Reddy and D. H. Robbins, Theories and computational models for composite laminates, Appl. Mech. Rev. **47**, 147–169 (1994).
[13] H. Altenbach, Theories for laminated and sandwich plates. A review, Mech. Compos. Mater. **34**, 243–252 (1998).
[14] S. A. Ambartsumian, Nontraditional theories of shells and plates, Appl. Mech. Rev. **55**, R35–R44 (2002).
[15] E. Carrera, Theories and finite elements for multilayered, anisotropic, composite plates and shells, Arch. Comput. Methods Eng. **9**, 1–60 (2002).
[16] J. N. Reddy, Mechanics of Laminated Composite Plates and Shells: Theory and Analysis (2nd edition) (CRC Press, Boca Raton, 2004).
[17] R. Kienzler, H. Altenbach, and I. Ott, (eds.) Theories of Plates and Shells: Critical Review and New Applications, (Springer-Verlag, Berlin, 2004).
[18] G. M. Kulikov and S. V. Plotnikova, Solution of static problems for a three-dimensional elastic shell, Dokl. Phys. **56**, 448–451 (2011).
[19] G. M. Kulikov and S. V. Plotnikova, On the use of a new concept of sampling surfaces in shell theory, Adv. Struct. Mater. **15**, 715–726 (2011).
[20] R. L. Burden and J. D. Faires, Numerical Analysis, ninth edition (Brooks/Cole, Cengage Learning, Boston, 2010).
[21] G. M. Kulikov and S. V. Plotnikova, Non-linear strain-displacement equations exactly representing large rigid-body motions. Part II: Enhanced finite element technique, Comput. Methods Appl. Mech. Eng. **195**, 2209–2230 (2006).
[22] G. M. Kulikov and S. V. Plotnikova, Non-linear geometrically exact assumed stress-strain four-node solid-shell element with high coarse-mesh accuracy, Finite Elem. Anal. Des. **43**, 425–443 (2007).
[23] G. M. Kulikov and S. V. Plotnikova, Equivalent single-layer and layer-wise shell theories and rigid-body motions. Part I: Foundations, Mech. Adv. Mater. Struct. **12**, 275–283 (2005).
[24] G. M. Kulikov and S. V. Plotnikova, Equivalent single-layer and layer-wise shell theories and rigid-body motions. Part II: Computational aspects, Mech. Adv. Mater. Struct. **12**, 331–340 (2005).
[25] B. F. Vlasov, On the bending of rectangular thick plate. Trans. Moscow State Univ. **2**, 25–31 (1957).
[26] T. K. Varadan and K. Bhaskar, Bending of laminated orthotropic cylindrical shells – an elasticity approach, Compos. Struct. **17**, 141–156 (1991).
[27] S. P. Timoshenko and J. N. Goodier, Theory of Elasticity, third edition (McGraw-Hill, New York, 1970).

